Carbohydrate Polymers 87 (2012) 524–530

Contents lists available at ScienceDirect

Carbohydrate Polymers

journal homepage: www.elsevier.com/locate/carbpol

Rheology and nanostructure of hydrophobically modified alginate (HMA) gels and solutions

Soumitra Choudhary, Surita R. Bhatia*

Department of Chemical Engineering, University of Massachusetts Amherst, Amherst, MA 01003 United States

ARTICLE INFO

Article history:
Received 24 February 2011
Received in revised form 4 August 2011
Accepted 5 August 2011
Available online 17 August 2011

Keywords:
Hydrophobically modified alginate
Amphiphilic biopolymer
Rheology
Associative polymer
Polysaccharide

ABSTRACT

The effect of hydrophobic modification on the mechanical and structural characteristics of hydrophobically modified alginate (HMA) solutions and hydrogels were evaluated. The HMA systems consisted of alkyl chains, C_8, grafted onto alginate backbones. With an increase in degree of substitution of hydrophobic tails, the association became stronger in solution, but same was not true for gels. The contribution of ionic crosslinking was found to be the dominant factor in determining the mechanical strength of hydrogels. Rheological measurements of 2 wt% HMA gels reveal formation of a strongly crosslinked network with an elastic modulus close to 100 kPa. Small-angle X-ray scattering (SAXS) experiments indicate that HMA assembles into a disordered structure with regions rich in the hydrophobic domain surrounded by a crosslinked hydrophilic network.

1. Introduction

Alginate is a hydrophilic polymer, which in aqueous media gets ionized carrying a negative charge on its backbone. The most popular method of crosslinking alginate is accomplished by crosslinking guluronic units of adjacent chains with divalent cations such as Ca^{2+}, Ba^{2+}, etc. (Augst, Kong, & Mooney, 2006). The initial mechanical strength and physical integrity of ionically crosslinked calcium gels tends to decrease over a period of time (De Boisseson et al., 2004) as the gels are exposed to aqueous media or monovalent cation such as Na^+. For long-term applications where retaining the structure is a necessity, this can be disadvantageous. One method of stabilizing alginate gels is to covert the alginate backbone into an amphiphilic polymer by attaching hydrophobic moieties to the chains. The hydrophilic portion makes the polymer water-soluble, while the hydrophobic domains tend to aggregate in aqueous solutions and form distinct structures with regions rich in hydrophilic and hydrophobic content. So, irrespective of whether calcium is leached out of the gels, the system is expected to remain physically intact due to these hydrophobic interactions.

Hydrophobic modification of alginate (HMA) has been found to enhance the stability of gels in water and other biological buffers containing calcium chelators, due to the attractive association among hydrophobic moieties in aqueous media (De Boisseson et al., 2004). The hydrophobic cavities formed could potentially be used as vehicles for the delivery of hydrophobic drugs. Similar to other associative polymers, above a critical concentration the clusters formed can span the whole sample space. The strength of the association can be tuned by varying degree of substitution (DS) and length/chemical nature of the hydrophobic tail (Colinet, Dulong, Hamaide, Le Cerf, & Picton, 2009; Knudsen, Lauten, Kjoniksen, & Nystrom, 2004; Leonard, De Boisseson, Hubert, Dalencon, & Dellacherie, 2004). However, it has been reported that the range and concentration within which strong hydrogels can be formed are limited (Leonard et al., 2004). Higher DS might render the polymer water-insoluble, whereas a lower value might have little effect on the properties. By suitably selecting the degree of hydrophobic substitution it is possible to retain the polyelectrolyte behavior of HMA. Hydrophobic groups attached to the polyelectrolyte backbone enable them to exhibit distinct characteristics, which are influenced by the interplay between hydrophobic association and electrostatic interaction.

Hydrophobically modified alginate, being a derivative of a biocompatible polymer, has a huge potential as a polymeric drug carrier (De Boisseson et al., 2004; Galant, Kjoniksen, Nguyen, Knudsen, & Nystrom, 2006; Leonard et al., 2004; Pelletier, Hubert, Lapicque, Payan, & Dellacherie, 2000; Colinet, Dulong, Mocanu, Picton, & Le Cerf, 2009). Previous studies of HMA have mainly been focused on its rheological and physicochemical properties in solution. Work on biomaterials applications of HMA has been limited, although it has been shown that different types of modified alginate can be used to deliver various proteins (De Boisseson et al., 2004; Yao, Ni, Xiong, Zhu, & Huang, 2010) and theophylline (Colinet, Dulong, Mocanu, et al., 2009) over extended periods of time.

* Corresponding author. Tel.: +1 413 545 0096; fax: +1 413 545 1647.
E-mail address: sbhatia@ecs.umass.edu (S.R. Bhatia).

0144-8617/$ – see front matter © 2011 Elsevier Ltd. All rights reserved.
doi:10.1016/j.carbpol.2011.08.025

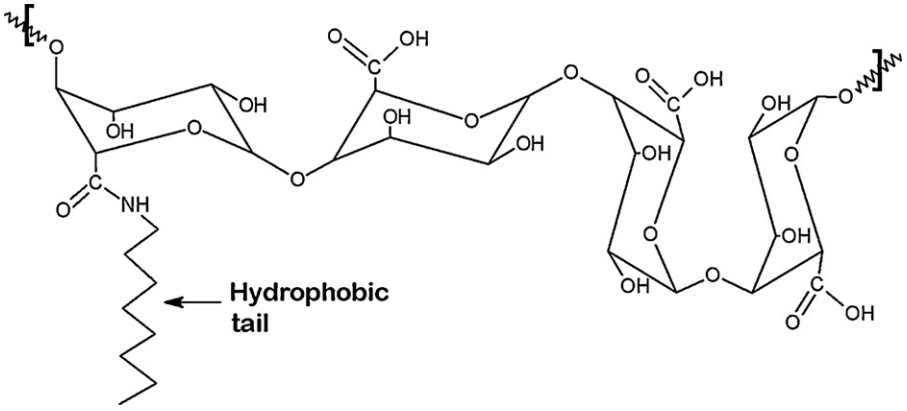

Fig. 1. Chemical structure of hydrophobically modified alginate.

In this article, we will discuss the rheological and small angle scattering characterization of HMA sol and gels in water. It will be seen that the material mechanical properties can be tuned by varying the degree of substitution of the hydrophobic group, and addition of crosslinker. Bulk rheology of modified alginate was performed to determine strength of the gels. HMA was synthesized by forming amide linkages between n-octylamine and carboxylate group present on the alginate backbone. The ability to alter the degree of substitution of hydrophobic groups and crosslinker density gave us an extra handle to tune the rheological and mechanical properties of the system. The effect of mechanical properties on drug release characteristics has also been studied and will be discussed in an upcoming publication.

2. Experimental

2.1. Materials

Sodium alginate, ethylene diamine tetra acetic acid (EDTA) and D-glucono-δ-lactone (GDL) were obtained from Sigma–Aldrich. The characteristics of the alginate as provided by the supplier are molecular weight range of 100,000–200,000; Mw of 120,000; and *G* content of 60–70%. Calcium chloride, 1-ethyl-3-(3-dimethyllaminopropyl) carbodiimide hydrochloride (EDC-HCl) and n-octyl amine was purchased from Fischer Scientific. All chemicals were of 99%+ pure ACS grade and used without further purification. All the solutions were prepared in nanopure water (resistivity < 18 MΩ cm).

2.2. HMA synthesis

Hydrophobically modified alginate was synthesized as per the procedure described in detail by Galant et al. (2006). In brief, 3 wt% aqueous alginate solution was acidified to pH ∼ 3.4 by adding 0.1 M HCl solution. The final concentration was adjusted to 2 wt% by adding water, if needed. To this solution the carboxyl activating agent 1-ethyl-3-(3-dimethylamino-propyl) carbodiimide was added and stirred for approximately 5 min. Octylamine (n-C_8) was added in stoichiometric amounts and stirred for another 24 h at ambient condition. After the completion of reaction the polymer was precipitated in acetone, and separated by centrifuging. To remove unreacted n-C_8 and any organic residue, HMA was further purified with acetone. Water-soluble and other low molecular weight impurities were removed by dialysis using a membrane with a molecular wt cutoff of 6000–8000, against nanopure water for 7 days. Finally, the product was recovered by freeze-drying (see HMA structure in Fig. 1). Different grades of HMA were prepared by changing the degree of substitution (DS), defined as number of alkyl substituent groups per monomer unit.

2.3. Polymer characterization

NMR spectra were collected on a Bruker 400 MHz instrument, obtained from D_20 solution at 85 °C. ^{1}H NMR spectra were referenced to residual $CHCl_3$ at 7.26 ppm. Viscosity measurements were performed using a standard Ubbelholde viscometer at a set temperature of 25 °C. Sizes of viscometers were selected such that efflux times were greater than 2 min to help eliminate error in readings. The solutions were filtered through 0.5 μm nylon filters to remove any large impurities. The samples were allowed to equilibrate for at least 20 min before taking the measurements.

2.4. Alkaline hydrolysis

A premeasured amount of HMA was dissolved in water and then treated with 0.4 N NaOH for ∼4 h (Pelletier et al., 2000). The alkali reaction breaks the amide bond, and hydrolyzes the alkyl group to alcohol, in our case, octanol. After the completion of reaction, 10 ml of toluene along with 0.015 ml of hexanol (internal reference) was added, and mixed vigorously by vortexing. The mixture was allowed to separate into organic and aqueous phases. The organic phase containing the released octanol was pipette out, and passed through 0.45 μm filter. The clarified mixture was analyzed through gas chromatography and mass-spectrometer system (GC–MS). The degree of substitution was calculated by comparing with a calibrated curve.

2.5. Sample preparation

Solutions of required concentration were prepared by dissolving polymer in nanopure water. Solutions were mechanically stirred for 24 h at ambient condition, and stored in refrigerator for couple of days at 4 °C for complete hydration. Pure alginate or its modified version was gelled by *in situ* release of calcium ions. The above technique slows the gelation rate, and gave us time to prepare sample of desired shape and size. It also resulted in homogenous gel across the entire cross section. Calcium–ethylene diamine tetra acetic acid (CaEDTA) complex was prepared by mixing equimolar amount of $CaCl_2$ and EDTA, the solution was neutralized by adding NaOH, and final concentration adjusted to 0.3 M with water. Gels were prepared by mixing HMA/alginate sol with CaEDTA followed by slow hydrolyzing GDL (Liu, Qian, Shu, & Tong, 2003). CaEDTA was added at 30% above the stoichiometric amount to crosslink all the guluronic units. Presence of high amount of counter ions (Na^+)

in CaEDTA thickens the HMA sol, hence the highest concentration of HMA gel (and sol) was set to be 2 wt%.

2.6. Rheological characterization

Small amplitude oscillatory shear studies were performed on a stress-controlled AR-G2 and AR-2000 rheometer by TA instruments. A measured amount of solution of stipulated concentration was directly transferred to the couette geometry. For gels, the final mixture (after the addition of GDL) was poured into the Teflon dish, and left for 48 h to complete the gelation. The disc-shaped samples of desired diameter was cut out from the middle of the dish to avoid rough edges, if any. Frequency sweeps were performed using parallel plate geometry. Stress sweeps were performed before the dynamic experiments to determine the range where G' and G'' were independent of the stress. Since the stress sweep was performed only at 1 Hz, the controlled stress in the frequency sweep was chosen from the mid tripartite of the linear viscoelastic regime. All the experiments were performed at 25 °C unless otherwise specified.

2.7. Small angle X-ray scattering (SAXS)

SAXS experiments were done using an in-house setup from Molecular Metrology Inc. (presently sold as Rigaku S-Max3000). It uses a 30 W microsource with a $30 \times 30\ \mu m^2$ spot size matched to a Maxflux® optical system (Osmic) leading to a low-divergence beam of monochromatic CuK_α radiation (wavelength $\lambda = 0.1542$ nm). After passing through series of guides and pinholes, the beam of about 0.4 mm diameter enters the sample chamber kept under vacuum. The scattered X-ray intensity was collected on a two-dimensional gas-filled wire detector at a distance of about 1500 mm from the sample. A beamstop of 4 mm diameter in the front protects the detector from high intensity direct beam. The beamstop has in its center a photodiode allowing monitoring the intensity of the direct beam. The angular range for SAXS (determined by the radius of the beamstop and of the detector) covers a wave vector range $0.06 < q < 1.6\ nm^{-1}$ where, $q = (4\pi/\lambda)\sin\theta$, 2θ being the scattering angle. This corresponds to dimensions between about 4 and 100 nm. The actual scattering angles were calibrated using the accurately known reflection from silver behenate. The samples were loaded in a sample holder pinhole, and sealed both sides with X-ray "transparent" Kapton tape. Experiments were run till the detector count rate was at least 1,00,000.

3. Results and discussion

3.1. Degree of substitution of amphiphilic derivatives

To determine the degree of substitution of hydrophobic groups onto polymer backbone ^1H NMR was performed. The NMR spectra displayed clear peaks corresponding to the octyl chain (data not shown), indicating that the substitution reaction was successful. However, the peaks in the spectra were broad, leading to uncertainty of 10–15% in the value of DS obtained from integrating the peaks. This phenomenon is usual with polymers above 80,000 molecular weight (Varum, Anthonsen, Grasdalen, & Smidsrod, 1991). The value of DS obtained for the targeted DS of 0.15 via NMR was approximately 0.13, and the value of DS obtained for the targeted DS of 0.30 via NMR was approximately 0.17; again, these values depend on correct integration of the peaks and have uncertainty of 10–15%.

To verify the DS from NMR with another analytical technique, the product was hydrolyzed with strong alkali and analyzed via GC–MS as described in Section 2.3. The targeted DS of 0.15 was found to be 0.14, and DS of 0.30 grade was found to be 0.18. They are designated as HMA-0.14 and HMA-0.18 respectively. These values agree fairly well with those obtained from NMR. For both samples, the measured DS was lower than expected from reaction stoichiometry, particularly for the sample targeting a DS of 0.30. As the reaction progresses and the DS increases, chains begin to associate and the solution viscosity increases. We suspect that either of these effects will decrease the efficiency of the grafting reaction, leading to a lower DS in the sample. As many authors (Pelletier et al., 2000) (Bu, Kjoniksen, Knudsen, & Nystrom, 2005) have noted in working on similar systems, that chemical analysis of these systems can be tricky and prone to errors, so there is an uncertainty of roughly 10–15% in the value of degree of substitution reported in this paper.

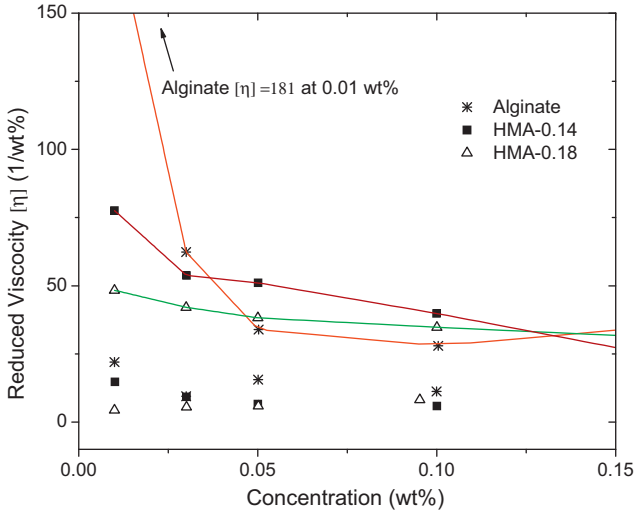

Fig. 2. Reduced viscosity of polymer solution at 25 °C vs concentration. Solutions prepared in water are connected by lines as a guide to the eyes. Unconnected data points are values of polymer solution in 0.1 M NaCl. *Y*-axis range is reduced to improve the resolution. (For interpretation of the references to colour in this figure legend, the reader is referred to the web version of this article.)

3.2. Viscosity at low concentration

Polyelectrolytes carrying ionizable groups exhibit a unique viscosity profile in dilute solution. At extremely dilute conditions, far below the concentration where entanglement can be an issue, the effective size of the molecule increases, defined by the Debye length. As a result there is a pronounced upturn in intrinsic viscosity at low concentration, termed the "electroviscous" effect (see alginate in water in Fig. 2). With increased concentration the charge on the polymer begins to become screened because of higher ionic strength, resulting in decreased viscosity with concentration. This feature of polyelectrolyte is typical and well documented (Knudsen et al., 2004; Konop & Colby, 1999; Nishida, Kaji, Kanaya, & Fanjat, 2002; Pavlov, Gubarev, Zaitseva, & Sibileva, 2006; Rabin, 1987).

We saw significantly lower intrinsic viscosity of HMA in water ($[\eta] = 77$ and 48 for DS of 0.14 and 0.18, respectively) as compared to alginate ($[\eta] = 181$) at the lowest concentration of 0.01 wt%. This may be due to the chain-breakage during synthesis at low pH, which would drops the molecular weight of HMA compared to alginate. Hydrophobically modified polyelectrolyte characteristics are governed by combination of hydrophobic and electrostatic interaction. Under dilute conditions, intramolecular bonds are favored, and as a result HM polymers may collapse and coalesce with each other. The presence of ionic charge on the polymer prevents hydrophobic groups to come closer due to electrostatic repulsion, and helps in stabilizing the solution. The interplay becomes interesting as the solution concentration increases from dilute to concentrated. A definite increase in the viscosity was observed for all grades of HMA

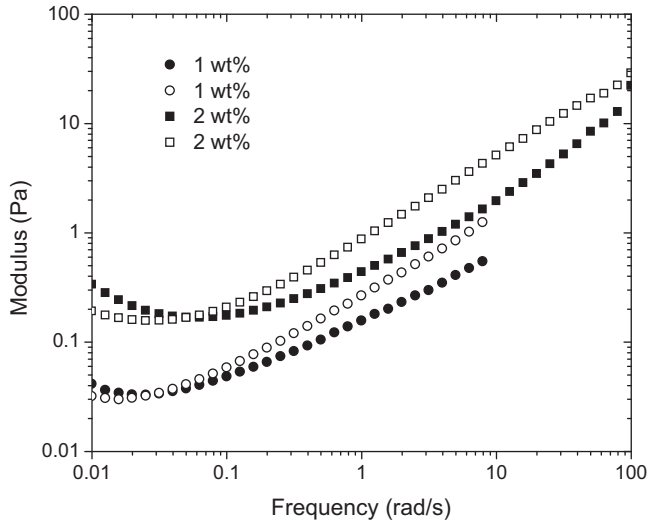

Fig. 3. Frequency sweep of HMA-0.14 solution at different concentration in water. Open symbols refer to viscous modulus (G''), and closed to elastic modulus (G').

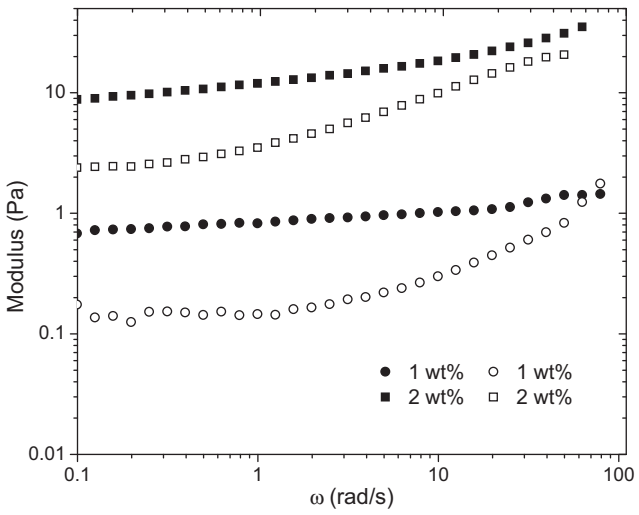

Fig. 4. Frequency sweep of HMA-0.18 solution at different concentration in water. Open symbols refer to viscous modulus (G''), and closed to elastic modulus (G').

over its precursor beyond 0.05 wt%, indicating the significance of hydrophobic association. At concentrations of 0.2 wt% and higher, the solution viscosity of unmodified alginate increases (data not shown), likely due to entanglement effects.

Between HMAs, the plot of reduced viscosity versus concentration was more dramatic for lower DS. The observed effect was in line with the phenomenon explained earlier. The polyelectrolyte effect is expected to be lower as the percentage of hydrophobic group increases (replacing the ionizable group with hydrophobic moiety). Thus it is possible to tune the viscoelastic and structural properties of the solution by varying the degree of hydrophobicity of the polymer. Samples using 0.1 M NaCl as the solvent showed no discernable trends at any concentration. The addition of salts to HMA solutions results in a significant drop in the reduced viscosity. The results indicate screening effect due to the addition of counterions. Among different polymer the values are practically the same.

3.3. Rheology

Dynamic mechanical analyses of both solution (sol) and gel samples were performed to determine elastic (G') and viscous (G'') modulus. The mechanical strength of the matrix has been known to have direct bearing on the drug delivery characteristics (Coviello et al., 2005; Woolfson, Malcolm, Campbell, Jones, & Russell, 2000). Since in majority of the cases it desirable to have controlled–release over an extended period of time, it is expected that higher mechanical strength should leads to better drug-eluding attributes. Microdomains are formed due to inter particle association driven by hydrophobic interaction and/or entanglement between the freely dangling polymer chains. Once the critical concentration is reached these interconnected domains can reach sample-spanning networks. The low mechanical strength of HMA-0.14 sol was probably due to either low overall polymer concentration or low substitution ratio. Fig. 3 shows the frequency sweep of HMA-0.14 solution at two different concentrations. In all cases, viscous forces were found to be dominant indicating weaker association. Stiffer gel-like behavior was seen at higher degree of substitution of 0.18 for all concentrations studied (Fig. 4).

The observed behavior can be attributed to associative network formation whose strength are directly related to number of elastically active junction as prescribed by Green and Tobolsky (1946). According to transient network theory developed by Green and Tobolsky (1946), the equilibrium modulus is proportional to the number of elastically effective chains per unit volume. Clearly, as the concentration of the junction points increases either due to higher DS or polymer content we see a higher modulus (Green & Tobolsky, 1946; Ng, Tam, & Jenkins, 2000; Pham, Russel, Thibeault, & Lau, 1999; Tanaka & Edwards, 1992). The frequency independent profile for HMA-0.18 solution gives some insight into the structure of the gels; the system has high density of crosslinked junctions that were initiated by hydrophobic interaction (Nystrom, Kjoniksen, Beheshti, Zhu, & Knudsen, 2009; Nystrom, Kjoniksen, & Iversen, 1999). These hydrophobic interactions trigger formation of clusters or aggregates that lead to three-dimensional networks.

Further information regarding the structure of the network can be deduced from the frequency sweep of loss tangent. In Fig. 5 we have plotted the tan δ versus frequency for HMA sol, and gels. For gels, tan δ should be invariant and that is what we observe for HMA gels (Fig. 5b). The interpretation of HMA-0.18 sol data in Fig. 5a

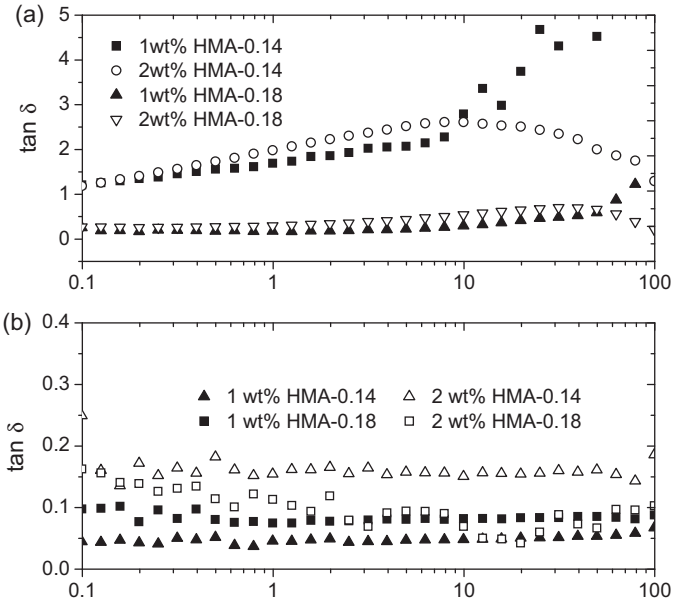

Fig. 5. tan δ value at different frequencies for HMA (a) HMA sol, (b) HMA gels. The x-axis in the graphs represents frequency in rad/s.

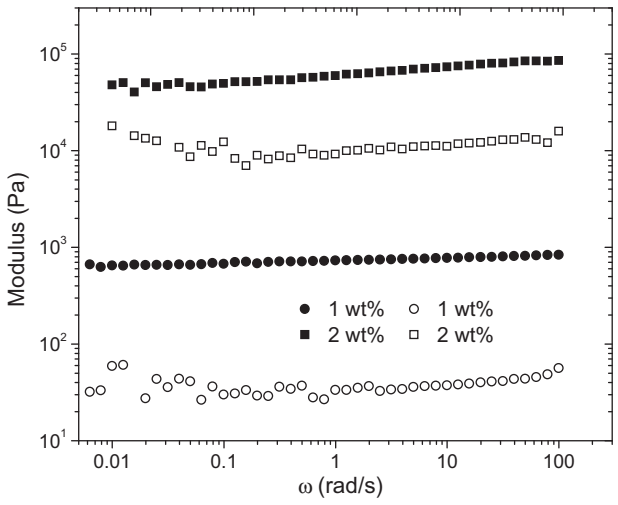

Fig. 6. Frequency sweep of HMA-0.14 gels at different concentration in water. Open symbols refer to viscous modulus (G''), and closed to elastic modulus (G').

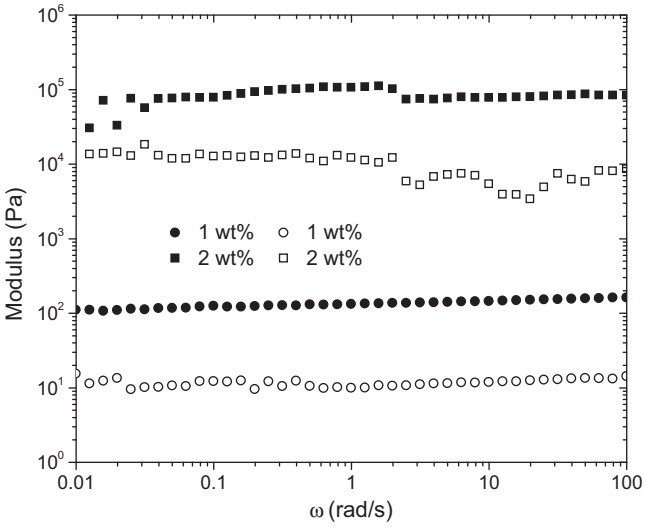

Fig. 7. Frequency sweep of HMA-0.18 gels at different concentration in water. Open symbols refer to viscous modulus (G''), and closed to elastic modulus (G').

is straightforward. Both the frequency sweep (Fig. 4) and tan δ profile (Fig. 5a) are consistent with the common notion. However, interesting results were seen for HMA-0.14 solution. The frequency sweep of HMA-0.14 sol (Fig. 3) indicates liquid-like behavior, but the loss tangent vs frequency plot (Fig. 5a) suggests characteristics similar to polymeric glasses made from poly (methyl methacrylate) and polystyrene (Larson, 1999). The anomaly is not clearly understood, perhaps the association under shear is short-lived or the system was still in the transient state; not sol but neither in gel state. An analogy can be drawn from the gelation kinetics of chemically crosslinked networks. The Winter–Chambon criterion (Winter & Chambon, 1986) was developed for systems undergoing a sol–gel transition from sol to gel, and has since been applied to several physically-crosslinked gels (Lin, Mallin, Chien, & Winter, 1991; Richtering, Gagnon, Lenz, Fuller, & Winter, 1992). While the sample is in the sol state, tan δ decreases with frequency, whereas it increases with frequency as the time crosses the gel point.

We can also interpret the rheology in terms of a characteristic relaxtion time, τ_m. Classic Maxwellian behavior with a single relaxation mode is only observed in a few associative polymer systems (Annable, Buscall, Ettelaie, & Whittlestone, 1993), inorganic glassy liquids (Sammler et al., 1996), and bulky non-polymer liquids at low frequencies (Larson, 1999). It is clear that the HMA-0.14 sol does not behaves as a typical Maxwell fluid, which indicates additional modes of stress relaxation. Nevertheless, we can estimate τ_m as the inverse of the crossover frequency, where $G'(\omega) = G''(\omega)$. From Fig. 3 it can be seen that τ_m increases with concentration. This can be due to increased entanglement or hydrophobic interaction with concentration (Castelletto, Hamley, Yuan, Kelarakis, & Booth, 2005; Pham et al., 1999; Serero et al., 1998; Tanaka & Edwards, 1992).

It is clear that significant improvement in mechanical strength was obtained due to hydrophobic substitution. Storage moduli for 2 wt% HMA gels were found to be close to 100 kPa (Figs. 6 and 7) compared to pure alginate gel at 2 wt%, where G' was in the order of 850 Pa. HMA gels are controlled by at least two type of interactions; one physical and the other chemically crosslinked. With increasing polymer content the contribution due to entanglement effects must also be considered. Moreover, the intrinsic viscosity data clearly demonstrate the polyelectrolyte effect on the solution properties. All of these contributions make the mechanism to understand the gel behavior even more complicated. It is important to note that CaEDTA solution contains large amount of counterions (Na^+), which were introduced while neutralization. Based upon our conclusion in Section 3.2 about the screening effect of counterions, it is intuitive to believe that polyelectrolyte effect on HMA gels should be minimal. From rheological characterization we found significant difference in G' between gels and sol, which indicate that chemical crosslinking with calcium ions plays a dominant role in determining the strength of the system. However, the two mechanisms, associative junctions and chemical crosslinking, were found to behave synergistically in improving the G'.

Major differences were observed in 1 wt% hydrogels, where HMA-0.14 sample had $G' \sim 700$ Pa as compared to $\sim$150 Pa for HMA-0.18. We would expect that number of ionizable groups would reduce progressively with the increase in DS. That would leave fewer sites to form complexes with divalent cations. As the number of permanent crosslinked junction decreases, so should the strength of the gels. Based on our previous conclusion regarding the dominant mechanism, this seems quite reasonable. Although 2 wt% HMA-0.14 gels were found to be slightly frequency dependent, the differences in G' between the different grades of Ca-HMA gels represented in Figs. 6 and 7 is trivial. That tells us in spite of the lower percentage of chemically crosslinked junctions in HMA-0.18 gels, above a certain concentration the effect of physical crosslinking due to hydrophobic interaction cannot be ignored. Unfortunately, addition of CaEDTA thickens the HMA solution that restricted us to the maximum gel concentration of 2 wt%. Overall, as far as the mechanical strength of Ca-HMA gel were concerned, the chemical crosslinking is significantly more important.

3.4. Small angle X-ray scattering

The polydispersity index (PDI) of the alginate prior to hydrophobic modification is 3–6, and we expect this to increase after modification. Moreover, the modification was random, and there was little to no control over attaching the hydrophobic moiety at a particular position. This would cause the HMA system to form irregular aggregates that does not conform to regular polymeric micelle (Castelletto, Hamley, & Pedersen, 2004; Goldmints, Yu, Booth, Smith, & Hatton, 1999; Huibers, Bromberg, Robinson, & Hatton, 1999; Tew, Sanabria-DeLong, Agrawal, & Bhatia, 2005). As a result we could not fit our data with form factor of established theoretical model. Hence all our efforts were focused on model-independent analysis of the scattering data.

SAXS profile of 1 and 2 wt% HMA sol and gel are shown in Fig. 8a and b. The spectra follows power law behavior in the q range

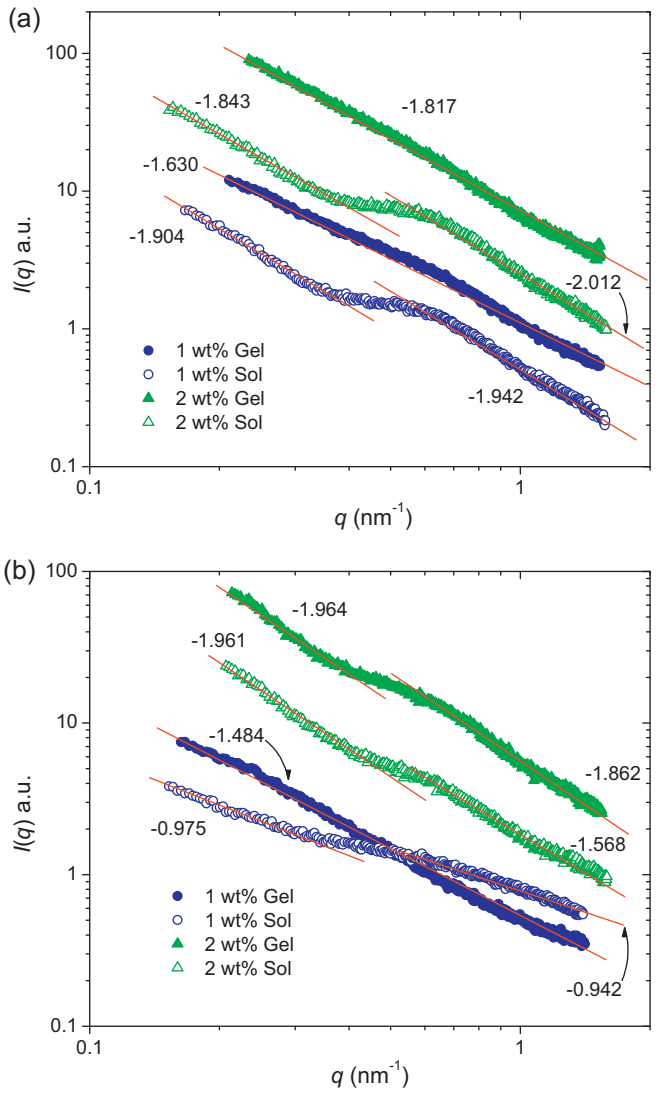

Fig. 8. Representation of SAXS spectra for (a) HMA-0.14, (b) HMA-0.18. The number on the graph denotes slope ($-\alpha$) from log–log plot of intensity vs scattering wave vector ($I(q) \sim q^{-\alpha}$). Some of the data are vertically shifted for clarity. (For interpretation of the references to colour in this figure legend, the reader is referred to the web version of this article.)

of ~0.15–1.55 nm^{-1}. The spectra are fitted according to the relation $I(q) \sim q^{-\alpha}$, the values of the exponent ($-\alpha$) are given in Fig 8a and b. This behavior is indicative of scattering from fractal objects (Beaucage, 1995; Bhatia, 2005). For mass fractals, mass 'M' is related to the radius of the structure, R as $M \sim R^{Df}$. The exponent 'D_f', called fractal dimension is equal to α, and can be used as a measure of network density (Beaucage, 1996). So, a value of 1 indicates "open" or loosely connected networks, and higher fractal exponent such as 3 suggests densely packed structure. If we consider surfaces with fractal dimension or surfaces coated with fractal materials, the relation is given by $S \sim R^{Ds}$, here the fractal exponents $Ds = 6 - \alpha$ (Higgins & Benoit, 1994). From the above relationship, the scattering exponent (α) should vary between 3 and 4 for materials with surface fractal characteristics.

Based on the above description and information from Fig. 8, it can be deduced that none of the gels or sols have compact structures with well-defined interfaces. The value of α varies from ~1 to 2, which corresponds to mass fractal value for rigid rod to lamellae/linear Gaussian chain/swollen branched polymer. The deviation from the power law scaling value of objects with "regular structure" make the analysis more challenging, although it is not totally unexpected. That said, several instances of arbitrary mass fractals dimension have been reported (Beaucage, 1996; Beaucage & Schaefer, 1994; Beaucage, Ulibarri, Black, & Schaefer, 1995; Hua, Anderson, Digregorio, Smith, & Beaucage, 1995), where it has been found that disordered materials do follow the unified exponential-power law equation developed by Beaucage et al. (1995). Also, the fact that a straight line in the log–log plot of I vs q was obtained over a reasonable q range gave us confidence to apply the above interpretation to our data.

The SAXS profile of HMA solution showed some interesting characteristics. At all concentrations and grades, we saw a discontinuity in the power law fit of $I(q) \sim q^{-\alpha}$. The spectra clearly indicate presence of distinct structure at two different length scales. The two regions are joined by a much shorter middle regime with relatively lower α value. Combining all the above information we can get some insight into the possible architecture; domains with dense structures connected or surrounded by a loose network. The absence of correlation peaks in I vs q plot shows no particular ordering of these domain. The domains were most likely formed due to hydrophobic interaction since they were absent from the pure alginate spectra (data not shown). The gel spectra, on the other hand, were mostly continuous over the entire q range except in the case of 2 wt% HMA-0.18. Clearly, addition of calcium ion disrupts the formation and a single exponent was found over entire q range. Comparing the exponent value of HMA-0.14 and HMA-0.18 we found it consistent with the rheological data; namely 1 wt% HMA-0.14 gel had higher G' over DS of 0.18, and also for other concentration or form (sol or gel). The denser structure is likely to yield higher storage modulus.

4. Conclusion

Hydrophobically modified alginate of different degree of substitution was prepared by a simple amide coupling reaction. These amphiphilic polymers were found to form stable gel-like networks in water due to associative hydrophobic interactions. The HMA sol can be further crosslinked with calcium to yield very high modulus hydrogels. The modulus of 2 wt% HMA gels was found to be of the order of 100 kPa, which is significant for a material with such high water content. There is a clear evidence of synergy between the two gelation mechanisms; an associative network driven by hydrophobic interaction and chemical crosslinking. However, the effect of chemical crosslinking was found to be more significant in determining bulk strength. SAXS studies show evidence of mass fractal structures at high to mid q. These systems do not seem to assemble into well-defined regular forms but rather arrange themselves into highly disordered structures as represented by the scattering spectra. The structural information from SAXS seems to correlate well with the bulk rheological properties.

Acknowledgments

We would like to acknowledge support from the NSF-funded Center for Hierarchical Manufacturing (CMMI-0531171 and CMMI-1025020) and use of central facilities of the NSF-funded MRSEC on Polymers (DMR-0820506) and the NSF-funded IGERT through the Institute of Cellular Engineering (DGE-0654128). The funding agencies had no role in the study design; in the collection, analysis and interpretation of data; in the writing of this paper; or in the decision to submit the paper for publication. Special thanks to Prof. S. Thayumanavan and group for assisting with synthesis and characterization of HMA and David Griffin for assisting with preparing manuscript figures.

References

Annable, T., Buscall, R., Ettelaie, R., & Whittlestone, D. (1993). The rheology of solutions of associating polymers – Comparison of experimental behavior with transient network theory. *Journal of Rheology*, *37*(4), 695–726.

Augst, A. D., Kong, H. J., & Mooney, D. J. (2006). Alginate hydrogels as biomaterials. *Macromolecular Bioscience*, *6*(8), 623–633.

Beaucage, G. (1995). Approximations leading to a unified exponential/power-law approach to small-angle scattering. *Journal of Applied Crystallography*, *28*, 717–728.

Beaucage, G. (1996). Small-angle scattering from polymeric mass fractals of arbitrary mass-fractal dimension. *Journal of Applied Crystallography*, *29*, 134–146.

Beaucage, G., & Schaefer, D. W. (1994). Structural studies of complex-systems using small-angle scattering – A unified guinier power-law approach. *Journal of Non-Crystalline Solids*, *172*, 797–805.

Beaucage, G., Ulibarri, T. A., Black, E. P., & Schaefer, D. W. (1995). Multiple size scale structures in silica–siloxane composites studied by small-angle scattering. *Hybrid Organic–Inorganic Composites*, *585*, 97–111.

Bhatia, S. R. (2005). Ultra-small-angle scattering studies of complex fluids. *Current Opinion in Colloid & Interface Science*, *9*(6), 404–411.

Bu, H. T., Kjoniksen, A. L., Knudsen, K. D., & Nystrom, B. (2005). Effects of surfactant and temperature on rheological and structural properties of semidilute aqueous solutions of unmodified and hydrophobically modified alginate. *Langmuir*, *21*(24), 10923–10930.

Castelletto, V., Hamley, I. W., & Pedersen, J. S. (2004). Small-angle neutron scattering study of the structure of superswollen micelles formed by a highly asymmetric poly(oxybutylene), âípoly(oxyethylene) diblock copolymer in aqueous solution. *Langmuir*, *20*(7), 2992–2994.

Castelletto, V., Hamley, I. W., Yuan, X. F., Kelarakis, A., & Booth, C. (2005). Structure and rheology of aqueous micellar solutions and gels formed from an associative poly(oxybutylene)–poly(oxyethylene)–poly(oxybutylene) triblock copolymer. *Soft Matter*, *1*(2), 138–145.

Colinet, I., Dulong, V., Hamaide, T., Le Cerf, D., & Picton, L. (2009). Unusual rheological properties of a new associative polysaccharide in salt media. *Carbohydrate Polymers*, *77*(4), 743–749.

Colinet, I., Dulong, V., Mocanu, G., Picton, L., & Le Cerf, D. (2009). New amphiphilic and pH-sensitive hydrogel for controlled release of a model poorly water-soluble drug. *European Journal of Pharmacuetics and Biopharmaceutics*, *73*(3), 345–350.

Coviello, T., Alhaique, F., Parisi, C., Matricardi, P., Bocchinfuso, G., & Grassi, M. (2005). A new polysaccharidic gel matrix for drug delivery: preparation and mechanical properties. *Journal of Controlled Release*, *102*(3), 643–656.

De Boisseson, M. R., Leonard, M., Hubert, P., Marchal, P., Stequert, A., Castel, C., et al. (2004). Physical alginate hydrogels based on hydrophobic or dual hydrophobic/ionic interactions: Bead formation, structure, and stability. *Journal of Colloid and Interface Science*, *273*(1), 131–139.

Galant, C., Kjoniksen, A. L., Nguyen, G. T. M., Knudsen, K. D., & Nystrom, B. (2006). Altering associations in aqueous solutions of a hydrophobically modified alginate in the presence of beta-cyclodextrin monomers. *Journal of Physical Chemistry B*, *110*(1), 190–195.

Goldmints, I., Yu, G. E., Booth, C., Smith, K. A., & Hatton, T. A. (1999). Structure of (deuterated PEO) (PPO) (deuterated PEO) block copolymer micelles as determined by small angle neutron scattering. *Langmuir*, *15*(5), 1651–1656.

Green, M. S., & Tobolsky, A. V. (1946). A new approach to the theory of relaxing polymeric media. *Journal of Applied Physics*, *17*(5), 407.

Higgins, J. S., & Benoit, H. C. (1994). *Polymers and neutrons scattering*. New York: Oxford University Press.

Hua, D. W., Anderson, J., Digregorio, J., Smith, D. M., & Beaucage, G. (1995). Structural-analysis of silica aerogels. *Journal of Non-Crystalline Solids*, *186*, 142–148.

Huibers, P. D. T., Bromberg, L. E., Robinson, B. H., & Hatton, T. A. (1999). Reversible gelation in semidilute aqueous solutions of associative polymers: A small-angle neutron scattering study. *Macromolecules*, *32*(15), 4889–4894.

Knudsen, K. D., Lauten, R. A., Kjoniksen, A. L., & Nystrom, B. (2004). Rheological and structural properties of aqueous solutions of a hydrophobically modified polyelectrolyte and its unmodified analogue. *European Polymer Journal*, *40*(4), 721–733.

Konop, A. J., & Colby, R. H. (1999). Polyelectrolyte charge effects on solution viscosity of poly(acrylic acid). *Macromolecules*, *32*(8), 2803–2805.

Larson, R. G. (1999). *The structure and rheology of complex fluids*. NY: Oxford University Press.

Leonard, M., De Boisseson, A. R., Hubert, P., Dalencon, F., & Dellacherie, E. (2004). Hydrophobically modified alginate hydrogels as protein carriers with specific controlled release properties. *Journal of Controlled Release*, *98*(3), 395–405.

Lin, Y. G., Mallin, D. T., Chien, J. C. W., & Winter, H. H. (1991). Dynamic mechanical measurement of crystallization-induced gelation in thermoplastic elastomeric poly(propylene). *Macromolecules*, *24*(4), 850–854.

Liu, X. X., Qian, L. Y., Shu, T., & Tong, Z. (2003). Rheology characterization of sol–gel transition in aqueous alginate solutions induced by calcium cations through in situ release. *Polymer*, *44*(2), 407–412.

Ng, W. K., Tam, K. C., & Jenkins, R. D. (2000). Lifetime and network relaxation time of a HEUR-C20 associative polymer system. *Journal of Rheology*, *44*(1), 137–147.

Nishida, K., Kaji, K., Kanaya, T., & Fanjat, N. (2002). Determination of intrinsic viscosity of polyelectrolyte solutions. *Polymer*, *43*(4), 1295–1300.

Nystrom, B., Kjoniksen, A. L., Beheshti, N., Zhu, K. Z., & Knudsen, K. D. (2009). Rheological and structural aspects on association of hydrophobically modified polysaccharides. *Soft Matter*, *5*(7), 1328–1339.

Nystrom, B., Kjoniksen, A. L., & Iversen, C. (1999). Characterization of association phenomena in aqueous systems of chitosan of different hydrophobicity. *Advances in Colloid and Interface Science*, *79*(2–3), 81–103.

Pavlov, G., Gubarev, A., Zaitseva, I., & Sibileva, M. (2006). Determination of intrinsic viscosity of polyelectrolytes in salt-free solutions. *Russian Journal of Applied Chemistry*, *79*(9), 1407–1412.

Pelletier, S., Hubert, P., Lapicque, F., Payan, E., & Dellacherie, E. (2000). Amphiphilic derivatives of sodium alginate and hyaluronate: Synthesis and physico-chemical properties of aqueous dilute solutions. *Carbohydrate Polymers*, *43*(4), 343–349.

Pham, Q. T., Russel, W. B., Thibeault, J. C., & Lau, W. (1999). Micellar solutions of associative triblock copolymers: The relationship between structure and rheology. *Macromolecules*, *32*(15), 5139–5146.

Rabin, Y. (1987). Anomalous viscosity of polyelectrolyte solutions. *Physical Review A*, *35*(8), 3579–3581.

Richtering, H. W., Gagnon, K. D., Lenz, R. W., Fuller, R. C., & Winter, H. H. (1992). Physical gelation of a bacterial thermoplastic elastomer. *Macromolecules*, *25*(9), 2429–2433.

Sammler, R. L., Otaigbe, J. U., Lapham, M. L., Bradley, N. L., Monahan, B. C., & Quinn, C. J. (1996). Melt rheology of zinc alkali phosphate glasses. *Journal of Rheology*, *40*(2), 285–302.

Serero, Y., Aznar, R., Porte, G., Berret, J. F., Calvet, D., Collet, A., et al. (1998). Associating polymers: From "flowers" to transient networks. *Physical Review Letters*, *81*(25), 5584–5587.

Tanaka, F., & Edwards, S. F. (1992). Viscoelastic properties of physically cross-linked networks – Transient network theory. *Macromolecules*, *25*(5), 1516–1523.

Tew, G. N., Sanabria-DeLong, N., Agrawal, S. K., & Bhatia, S. R. (2005). New properties from PLA–PEO–PLA hydrogels. *Soft Matter*, *1*(4), 253–258.

Varum, K. M., Anthonsen, M. W., Grasdalen, H., & Smidsrod, O. (1991). High-field Nmr-spectroscopy of partially N-deacetylated chitins (chitosans). 1. Determination of the degree of N-acetylation and the distribution of N-acetyl groups in partially N-deacetylated chitins (chitosans) by high-field NMR-spectroscopy. *Carbohydrate Research*, *211*(1), 17–23.

Winter, H. H., & Chambon, F. (1986). Analysis of linear viscoelasticity of a cross-linking polymer at the gel point. *Journal of Rheology*, *30*(2), 367–382.

Woolfson, A. D., Malcolm, R. K., Campbell, K., Jones, D. S., & Russell, J. A. (2000). Rheological, mechanical and membrane penetration properties of novel dual drug systems for percutaneous delivery. *Journal of Controlled Release*, *67*(2–3), 395–408.

Yao, B. L, Ni, C. H., Xiong, C., Zhu, C. P., & Huang, B. (2010). Hydrophobic modification of sodium alginate and its application in drug controlled release. *Bioprocess and Biosystems Engineering*, *33*(4), 457–463.